Preprint Title	Selective Mono-Formylation of Naphthalene-Fused Propellanes for Methylene-Alternating Copolymers
Authors	Kenichi Kato, Tatsuki Hiroi, Seina Okada, Shunsuke Ohtani and Tomoki Ogoshi
Publication Date	15 Apr. 2025
Article Type	Full Research Paper
Supporting Information File 1	SupportingInformation.pdf; 18.4 MB
ORCID® iDs	Kenichi Kato - https://orcid.org/0000-0001-5348-5521

Selective Mono-Formylation of Naphthalene-Fused Propellanes for Methylene-Alternating Copolymers

Kenichi Kato*[1], Tatsuki Hiroi[1], Seina Okada[1], Shunsuke Ohtani[1] and Tomoki Ogoshi*[1,2]

Address: [1]Department of Synthetic Chemistry and Biological Chemistry, Graduate School of Engineering, Kyoto University, Katsura, Nishikyo-ku, Kyoto, 615-8510, Japan and [2]WPI Nano Life Science Institute, Kanazawa University, Kakuma-machi, Kanazawa, 920-1192, Japan

Email: Kenichi Kato – katok@sbchem.kyoto-u.ac.jp; Tomoki Ogoshi – ogoshi@sbchem.kyoto-u.ac.jp

* Corresponding author

Abstract

Development of three-dimensional (3D) building blocks is a key to change tight molecular assemblies of rigid π-conjugated planes into organic functional materials endowed with molecular-size cavities. To increase the diversity of available 3D building blocks, we herein report electrophilic formylation of naphthalene-fused [3.3.3]- and [4.3.3]propellanes as the first selective single-point functionalization by virtue of through-space electronic communications between the naphthalene units. The propellane skeletons have well-defined 3D structures and moderate flexibility at the same time. Therefore, the mono-formyl products are good precursors for soft materials which show molecular-size cavities and require de-symmetrized building blocks. As a

proof of concept, methylene-alternating copolymers were prepared by reduction to corresponding alcohols and following acid-mediated condensation. The linear co-polymers show good solubility and carbon dioxide adsorption.

Keywords

formylation; building block; alternating copolymer; gas adsorption; propellane

Introduction

Combination of sp^2- and sp^3-hybridized atoms in core π-skeletons [1] is a key to go beyond common organic functional materials composed of rigid π-conjugated planes and flexible peripheral substituents. Because larger π-conjugated planes mostly display low solubility and dense packing due to the π/π stacking and CH/π interactions, surrounding alkyl and other flexible moieties are widely adopted to improve the solubility and modulate the molecular assemblies [2]. By contrast, the presence of sp^3-hybridized atoms in core π-skeletons can lead to three-dimensional (3D) structures with appropriate rigidity, thereby giving macrocyclic arenes [3], molecule-based cages and frameworks [4,5], polymers of intrinsic microporosity [6], and so forth. Characteristically, they possess molecular-size cavities, which contribute to intricate molecular recognition [7], confined spaces for reactions [8], and small-molecule storage and transport [9]. Further progress in such unique organic materials largely depends on the exploitation of 3D π-building blocks. However, the variety of building blocks are limited to a few families such as tetraphenylmethane and triptycene [10,11]. Widespread use of 3D π-skeletons requires not only efficient construction of the skeletons but also functionalization with precise control of substitution numbers and positions. Along this line, fully π-fused [4.4.4]- and [3.3.3]propellanes [12] were able to

be brominated and nitrated at six positions while retaining molecular symmetry (Figure 1) [13,14,15]. One functional group was selectively introduced to each naphthalene ring of fully π-fused [4.3.3]- and [3.3.3]propellane, **[4.3.3]** and **[3.3.3]**, respectively [16,17,18a]. In this work, we report introduction of a single functional group to a whole skeleton of **[4.3.3]** and **[3.3.3]**, using formylation [18]. The reaction was electrophilic, and the substrates are effectively deactivated toward further reactions upon introduction of an electron-withdrawing formyl group because of through-space electronic interactions between the naphthalene units. The mono-formyl products are reduced to corresponding alcohols, which are reacted in Friedel–Crafts conditions. Amorphous methylene-alternating copolymers are obtained without particular macrocyclic oligomers. Due to the 3D components, the linear copolymers display good solubility in $CHCl_3$ and THF and adsorption properties for CO_2 gas.

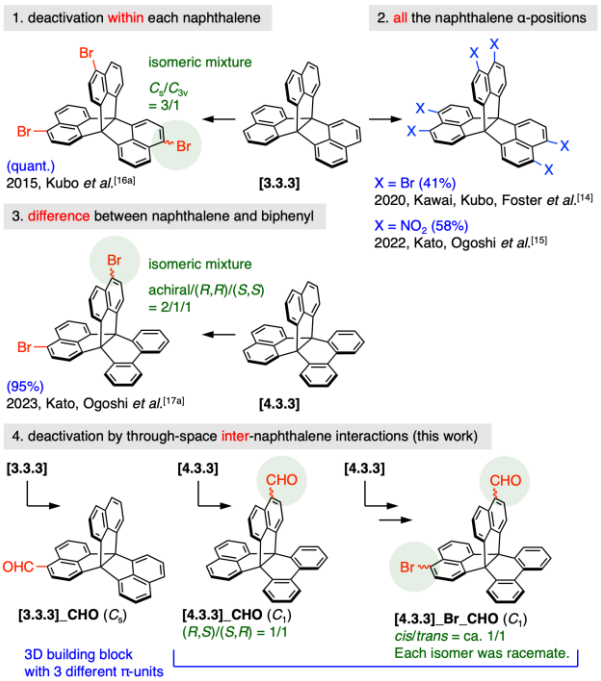

Figure 1: Chemical structures of fully π-fused propellanes and their typical reaction patterns toward electrophilic functionalization.

Results and Discussion

Selective mono-formylation

Initially, we tried introducing formyl groups into a fully π-fused [4.3.3]propellane via organometal species, which had been effective for functional π-extended systems [19]. This scheme also enables control of the number of formyl groups by starting materials and reagents. Brominated [4.3.3]propellane was reacted with *n*-BuLi or *i*-PrMgCl·LiCl to generate organometal species, which was quenched with *N*,*N*-dimethylformamide (DMF) as an electrophile (Table S201 in Supporting Information, SI). Despite several trials, the reactions led to complicated mixtures owing to decomposition and de-bromination or predominant recovery of the starting material, respectively.

Then, we turned our attention to electrophilic formylation. Vilsmeier–Haack [20] and Duff [21] reactions led to recovery of starting material or a complicated mixture probably owing to the modestly electron-rich and sterically demanding naphthalene α-positions (Table S202, entry 1–3). By contrast, a combination of dichloromethyl methyl ether and $TiCl_4$ (Rieche reaction) [18,22] yielded mono-formyl product, **[4.3.3]_CHO**, in a selective manner (Table 1, entry 1). To suppress decomposition in the overnight reaction at room temperature, the reaction time was reduced to 1.5 h, which afforded **[4.3.3]_CHO** in isolated yield of 80% (entry 2). The same protocol was successfully applicable to pristine π-fused [3.3.3]propellane **[3.3.3]**, giving **[3.3.3]_CHO** selectively in 67% yield (entry 3).

Table 1: Formylation of naphthalene-fused propellanes.

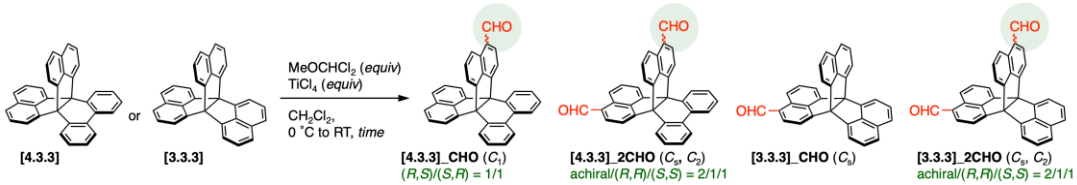

entry	*substrate*	*equiv*	*time*	results
1	**[4.3.3]**	1.25	29 h	**[4.3.3]_CHO** (48%)
2	**[4.3.3]**	1.2	1.5 h	**[4.3.3]_CHO** (80%), **[4.3.3]** (18%)
3	**[3.3.3]**	1.2	1.5 h	**[3.3.3]_CHO** (67%), **[3.3.3]** (12%), **[3.3.3]_2CHO** (5.1%)
4	**[3.3.3]**	2.4	1.5 h	**[3.3.3]_2CHO** (25%), **[3.3.3]_CHO** (61%)
5	**[4.3.3]**	2.4	1.5 h	**[4.3.3]_2CHO** (1.8%), **[4.3.3]_CHO** (56%)
6	**[4.3.3]**	2.4	18 h	**[4.3.3]_2CHO** (9.9%), **[4.3.3]_CHO** (33%)
7[a]	**[4.3.3]_Br**	1.2	18 h	**[4.3.3]_Br_CHO** (39% in 2 steps from **[4.3.3]**)

[a]*Substrate* was a 1:2:1 mixture of **[4.3.3]**, **[4.3.3]_Br**, and **[4.3.3]_2Br**, obtained by bromination of **[4.3.3]** with 1.03 equiv of Br_2 (Figure S201) [17a].

In electrophilic aromatic substitution, multi-fold reactions are possible, and the number of substitution is sometimes difficult to control by tuning reaction temperature and time. Indeed, bromination of **[3.3.3]** and **[4.3.3]** was reported as three/six- and two-fold reactions, respectively [14,16a,17a]. If the amount of bromine was limited, resulting nearly random mixtures of brominated compounds would be practically impossible to separate by chromatography on silica gel because of their low polarity and poor solubility in *n*-hexane. Nitration of **[3.3.3]** gave solely six-fold nitrated product due to low solubility of the starting material [15]. The current reaction is the first practical method for selective mono-functionalization of **[3.3.3]** and **[4.3.3]**, to the best of our knowledge. It is also noteworthy that this reaction further de-symmetrized the

[4.3.3]propellane skeleton of **[4.3.3]** into a 3D building block bearing three different fused π-units.

Di-formylation and computed electronic structures

In the formylation of **[3.3.3]**, di-formylated product **[3.3.3]_2CHO** was obtained in 5.1% yield. In expectation of successful multi-fold formylation, the equivalents of dichloromethyl methyl ether and $TiCl_4$ were doubled (entry 4). The yield of **[3.3.3]_2CHO** modestly increased to 25% with a slight decrease in the yield of **[3.3.3]_CHO** (61%). Although further increase of the equivalents and prolonged reaction time may provide more **[3.3.3]_2CHO**, total amount of the formulated products seemed to be almost maximized in this entry because of the competing decomposition in this strongly acidic conditions. In the case of **[4.3.3]**, di-formylation gave only 1.8% of **[4.3.3]_2CHO** after 1.5 h (entry 5), which was consistent with the absence of **[4.3.3]_2CHO** in mono-formylation. Due to the low reactivity, the reaction time was elongated to 18 h (entry 6). The yield of **[4.3.3]_2CHO** was improved to 9.9%, whereas the yield of **[4.3.3]_CHO** decreased to 33% owing to competing decomposition (entry 7). As a substrate, a mixture obtained by mono-bromination of **[4.3.3]** could be used, giving difunctional building block **[4.3.3]_Br_CHO** in 39% yield. The reaction was highly successful because the bromination gave a nearly random 1:2:1 mixtures of **[4.3.3]**, **[4.3.3]_Br** and **[4.3.3]_2Br**.

To gain insight into the different reactivity between **[3.3.3]** and **[4.3.3]**, theoretical calculations were performed at the ωB97X-D/6-31G(d,p) level (Figure S901–S903). Although distribution of the highest occupied molecular orbitals (HOMOs) was similarly delocalized to multiple naphthalene units, the energy for **[3.3.3]** (−7.23 eV) was higher than that of **[4.3.3]** (−7.32 eV). Upon formylation, the HOMO energies of **[3.3.3]** and

[4.3.3] were stabilized to −7.44 eV and −7.55 eV by 0.21 eV and 0.23 eV, respectively. These values accorded with the observed reactivities and selectivity well.

Attempted macrocyclization leading to linear polymers

Formyl groups have diverse reactivities and enable facile condensation, dynamic covalent chemistry, and so on. In this work, we tried synthesis of cyclic oligomers composed of naphthalene-fused propellanes simply by reduction into corresponding alcohols and following acid-mediated Friedel–Crafts-type reactions (Figure 2a, S201) [23]. Reduction by $NaBH_4$ proceeded well for both mono-aldehydes, **[4.3.3]_CHO** and **[3.3.3]_CHO**, over 90% yield. Alcohol products, **[4.3.3]_CH_2OH** and **[3.3.3]_ CH_2OH**, were then tested in acidic conditions using anhydrous $FeCl_3$ as a Lewis acid. After the reactions, alcohol proton signals at 1.54–1.58 ppm disappeared in the ^{1}H NMR spectra, and aliphatic carbon ones at 63.14–63.20 ppm were largely up-field-shifted to ca. 34 ppm in the ^{13}C NMR spectra due to conversion to methylene groups (Figure 2b, S315, S316). However, all the ^{1}H NMR signals were broad, and gel permeation chromatography (GPC) charts indicated broad patterns due to multiple products with varying molecular weights. These results implied that formation of well-defined cyclic oligomers was quite limited. To increase the well-defined species, **[4.3.3]_CH_2OH** was separated into two enantio-pure fractions (Figure S505), one of which was used for the acid-mediated reaction. Despite the stereo-controlled substrate, ^{1}H NMR spectrum of the product remained broad. Therefore, we concluded that these systems were difficult to give specific macrocyclic oligomers but instead provided linear polymers composed of fully π-fused propellanes.

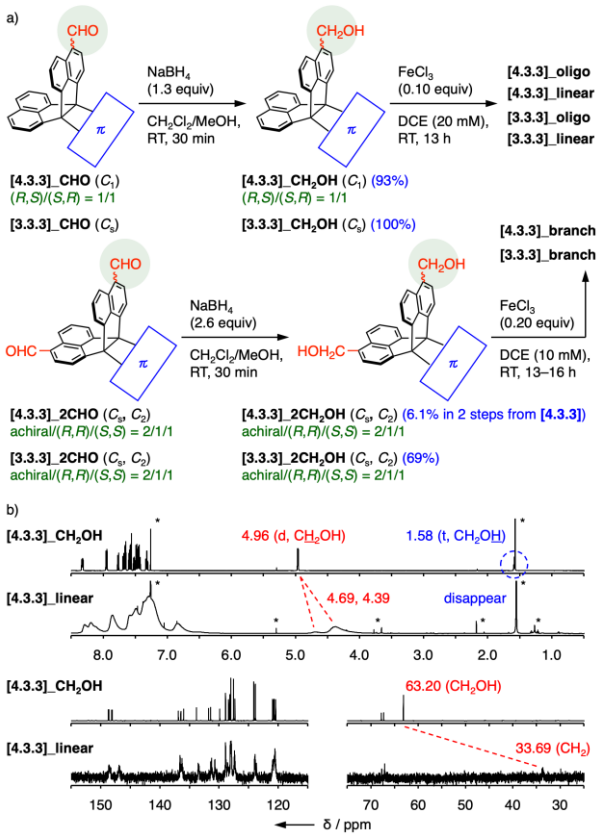

Figure 2: a) Synthesis of methylene-alternating copolymers of fully π-fused propellanes. DCE, 1,2-dichloroethane. b) ^{1}H (500 MHz, top) and ^{13}C (126 MHz, bottom) NMR spectra of **[4.3.3]_CH$_2$OH** and **[4.3.3]_linear** in $CDCl_3$ at room temperature.

After the reactions, each product was separated into oligomer and linear polymer by preparative GPC using $CHCl_3$ as eluent. According to analytical GPC in THF (Figure S501–504), oligomer fractions were mainly composed of tetramer for **[3.3.3]_oligo** and dimer and trimer for **[4.3.3]_oligo**. Fractions of linear polymers indicated peaktop molecular weights at around octamer for **[3.3.3]_linear** and pentamer and hexamer for **[4.3.3]_linear** (see also Table 2). In analogy with mono-aldehydes, di-aldehydes were reduced to di-alcohols, **[3.3.3]_2CH$_2$OH** and **[4.3.3]_2CH$_2$OH**, and polymerized in acidic conditions (Figure 2a). Insoluble solids, **[3.3.3]_branch** and **[4.3.3]_branch**, were obtained due to formation of bonding networks and washed repeatedly with CH_2Cl_2, H_2O, and acetone.

Table 2: Properties of methylene-alternating copolymers[a].

	M_n	M_w	M_w/M_n	T_{90} [°C]	CY [wt%]	V (CO_2) [$cm^3\ g^{-1}$]	S_{BET} [$m^2\ g^{-1}$]
[3.3.3]_oligo	–	–	–	532	76	22	–
[3.3.3]_linear	3.29×10^3	3.79×10^3	1.15	528	68	24	–
[3.3.3]_branch	–	–	–	415	64	18	61
[4.3.3]_oligo	–	–	–	468	47	15	–
[4.3.3]_linear	2.69×10^3	3.16×10^3	1.17	491	46	15	–
[4.3.3]_branch	–	–	–	543	75	29	323

[a]M_n, number-average molar mass; M_w, mass-average molar mass; T_{90}, temperature at which weight loss reaches 10%; CY, carbonization yield; V (CO_2), CO_2 uptake (STP) at 90 kPa; S_{BET}, BET surface area

Characterization of methylene-alternating copolymers

Thermal stability of the oligomers and polymers were evaluated with thermogravimetric analysis (TGA) (Figure S703). Temperatures at which weight loss reached 10% (T_{90}) were 468–491 °C and carbonization yields at 900 °C (CY) were ca. 46wt% for **[4.3.3]_oligo** and **[4.3.3]_linear**. T_{90} and CY of **[4.3.3]_branch** showed higher values of 543 °C and 75 wt% probably owing to the network structure. By contrast, soluble **[3.3.3]_oligo** and **[3.3.3]_linear** had relatively high T_{90} of 528–532 °C and CY of 68–76 wt%. The high values were ascribed to two unsubstituted naphthalene rings in precursor **[3.3.3]_CH_2OH**, which caused facile branching in the reaction or heating process. T_{90} and CY of **[3.3.3]_branch** (415 °C and 64 wt%) were lower than those of **[3.3.3]_linear** because of two-step decay profile (Figure S703a).

All the samples showed broad powder X-ray diffraction (PXRD) patterns with unclear peaks at around 2θ = 11° and 20° (Figure S601) and continuous curves in differential scanning calorimetry (DSC) between –70 and 300 °C (Figure S701, S702). The results indicated that the polymers were amorphous while giving relatively high thermal stability toward phase transition and decomposition.

Then, gas adsorption properties [15,24] were evaluated after the samples were activated in vacuo at 120 °C (Figure 3, S801, S802). Their chemical structures did not necessarily contain branched or ladder-type connections, but all of them displayed CO_2 adsorption properties at 298 K probably due to the 3D components. The uptake values at standard temperature and pressure (STP) were 15–29 $cm^3\ g^{-1}$ at 90 kPa. In this series, a sample with higher T_{90} and CY values tended to exhibit a higher adsorption capacity for CO_2. By contrast, the linear oligomers and polymers did not adsorb N_2 gas at 77 K. The adsorption isotherms of branched polymers did not have major IUPAC type-I contributions either, indicating the absence of micropores suitable for N_2 adsorption. The curve for **[3.3.3]_branch** looked like type-II, and that of **[4.3.3]_branch** showed multistep uptake. In the desorption step, both samples retained most of the adsorbed N_2 molecules even at 30 kPa. These observations and slow equilibrium in the adsorption processes suggested that presence of narrow connections between molecular-size cavities disturbed smooth N_2 adsorption and desorption. Molecular design for uniform microporosity and efficient polymerization is a next challenge.

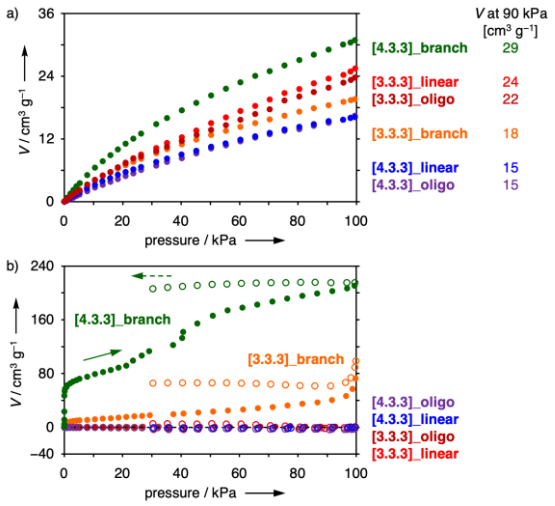

Figure 3: Gas adsorption (filled circles) and desorption (open circles) isotherms of **[3.3.3]_oligo** (dark red), **[3.3.3]_linear** (red), **[3.3.3]_branch** (orange), **[4.3.3]_oligo** (purple), **[4.3.3]_linear** (blue), and **[4.3.3]_branch** (green). a) CO_2 at 298 K and b) N_2 at 77 K.

Conclusion

In this work, we developed formylation on a naphthalene rings in [3.3.3]- and [4.3.3]-type fully π-fused propellanes. High selectivity was achieved for mono formylation on a naphthalene ring. It was reported that bromination proceeded in three- or six-fold manners for a [3.3.3]propellane [14,16], and in two-fold one for a [4.3.3]propellane [17]. Nitration of the [3.3.3]propellane also yielded an exclusive six-fold product [15]. The current formylation is valuable as the first reliable method for mono-functionalization of naphthalene-fused propellanes without giving inseparable mixtures with multi-functionalized products. Due to the wide reactivities of formyl group, the mono-formyl propellanes would promote new research domains on non-branched linear polymers, macrocyclic compounds, and molecular assemblies that incorporate propellanes as key 3D components. As a proof of concept, the formylated products were reduced to

corresponding alcohols and polymerized in acidic conditions. Although the degrees of polymerization were not high, the methylene-alternating copolymers displayed gas adsorption properties. Further studies are underway to novel functional materials containing fully π-fused propellanes as flexible 3D building blocks.

Supporting Information

Supporting information includes general information, synthetic procedures and compound data, NMR and MS spectra, HPLC charts, and results of PXRD, DSC, TGA, gas adsorption, and theoretical calculations.

Supporting Information File 1:

File Name: SupportingInformation.pdf

File Format: PDF

Title: Supporting Information

Acknowledgements

The authors acknowledge Dr. Takeshi Yamamoto and Prof. Dr. Michinori Suginome of Kyoto University for PXRD measurement.

Funding

This work was supported by JSPS KAKENHI Grant Numbers JP21K14611 (Early-Career Scientists, K.K.), JP23H04027 (Transformative Research Areas (A), K.K.), JP25K18019 (Early-Career Scientists, K.K.), and JP22H00334 and JP25H00896 (Scientific Research (A), T.O.), and MEXT World Premier International Research Center Initiative (WPI), Japan. K.K. acknowledge Tokuyama Science Foundation and Yazaki Memorial Foundation for Science and Technology.

References

1. Representative examples of 3D materials: a) Seiki, N.; Shoji, Y.; Kajitani, T.; Ishiwari, F.; Kosaka, A.; Hikima, T.; Takata, M.; Someya, T.; Fukushima, T. *Science* **2015**, *348*, 1122–1126; b) Ma, T.; Kapustin, E. A.; Yin, S. X.; Liang, L.; Zhou, Z.; Niu, J.; Li, L.-H.; Wang, Y.; Su, J.; Li, J.; Wang, X.; Wang, W. D.; Wang, W.; Sun, J.; Yaghi, O. M. *Science* **2018**, *361*, 48–52; c) Koner, K.; Karak, S.; Kandambeth, S.; Karak, S.; Thomas, N.; Leanza, L.; Perego, C.; Pesce, L.; Capelli, R.; Moun, M.; Bhakar, M.; Ajithkumar, T. G.; Pavan, G. M.; Banerjee, R. *Nat. Chem.* **2022**, *14*, 507–514.

2. a) Rehahn, M.; Schlüter, A.-D.; Wegner, G. *Polymer* **1989**, *30*, 1054–1059; b) Rehahn, M.; Schlüter, A.-D.; Wegner, G. *Polymer* **1989**, *30*, 1060–1062; c) Remmers, M.; Müller, B.; Martin, K.; Räder, H.-J. *Macromolecules* **1999**, *32*, 1073–1079; d) Tsuda, A.; Osuka, A. *Science* **2001**, 293, 79–82; e) Aratani, N.; Takagi, A.; Yanagawa, Y.; Matsumoto, T.; Kawai, T.; Yoon, Z. S.; Kim, D.; Osuka, A. *Chem. Eur. J.* **2005**, *11*, 3389–3404; f) Rieger, R.; Müllen, K. *J. Phys. Org. Chem.* **2010**, *23*, 315–325.

3. a) Liu, Z.; Nalluri, S. K. M.; Stoddart, J. F. *Chem. Soc. Rev.* **2017**, *46*, 2459–2478; b) Han, X.-N.; Han, Y.; Chen, C.-F. *Chem. Soc. Rev.* **2023**, *52*, 3265–3298.

4. a) Little, M. A.; Cooper, A. I. *Adv. Funct. Mater.* **2020**, *30*, 1909842; b) Zhang, G.; Hua, B.; Dey, A.; Ghosh, M.; Moosa, B. A.; Khashab, N. M. *Acc. Chem. Res.* **2021**, *54*, 155–168.

5. a) El-Kaderi, H. M.; Hunt, J. R.; Mendoza-Cortés, J. L.; Côté, A. P.; Taylor, R. E.; O'Keeffe, M.; Yaghi, O. M. *Science* **2007**, *316*, 268–272; b) Geng, K.; He, T.; Liu, R.; Dalapati, S.; Tan, K. T.; Li, Z.; Tao, S.; Gong, Y.; Jiang, Q.; Jiang, D. *Chem. Rev.* **2020**, *120*, 8814–8933; c) Tian, Y.; Zhu, G.; *Chem. Rev.* **2020**, *120*, 8934–8986; d) Hisaki, I.; Xin, C.; Takahashi, K.; Nakamura, T. *Angew. Chem. Int. Ed.* **2019**, *58*, 11160–11170; e) Li, Z.-T.; Yu, S.-B.; Liu, Y.; Tian, J.; Zhang, D.-W. *Acc. Chem. Res.* **2022**, *55*, 2316–

2325; f) Ami, T.; Oka, K.; Tsuchiya, K.; Tohnai, N. *Angew. Chem. Int. Ed.* **2022**, *61*, e202202597.

6. a) Budd, P. M.; Ghanem, B. S.; Makhseed, S.; McKeown, N. B.; Msayib, K. J.; Tattershall, C. E. *Chem. Commun.* **2004**, 230–231; b) Budd, P. M.; Elabas, E. S.; Ghanem, B. S.; Makhseed, S.; McKeown, N. B.; Msayib, K. J.; Tattershall, C. E.; Wang, D. *Adv. Mater.* **2004**, *16*, 456–459; c) Budd, P. M.; McKeown, N. B.; Fritsch, D. *J. Mater. Chem.* **2005**, *15*, 1977–1986; d) Carta, M.; Malpass-Evans, R.; Croad, M.; Rogan, Y.; Jansen, J. C.; Bernardo, P.; Bazzarelli, F.; McKeown, N. B. *Science* **2013**, *339*, 303–307; e) Ghanem, B. S.; Swaidan, R.; Litwiller, E.; Pinnau. I. *Adv. Mater.* **2014**, *26*, 3688–3692.

7. Guo, C.; Sedgwick, A. C.; Hirao, T.; Sessler, J. L. *Coord. Chem. Rev.* **2021**, *427*, 213560.

8. Grommet, A. B.; Feller, M.; Klajn, R. *Nat. Nanotechnol.* **2020**, *15*, 256–271.

9. a) Zou, L.; Sun, Y.; Che, S.; Yang, X.; Wang, X.; Bosch, M.; Wang, Q.; Li, H.; Smith, M.; Yuan, S.; Perry, Z.; Zhou, H.-C. *Adv. Mater.* **2017**, *29*, 1700229; b) Huang, T.; Alyami, M.; Kashab, N. M.; Nunes, S. P. *J. Mater. Chem. A* **2021**, *9*, 18102–18128; c) Zhang, R.; Daglar, H.; Tang, C.; Li, P.; Feng, L.; Han, H.; Wu, G.; Limketkai, B. N.; Wu, Y.; Yang, S.; Chen, A. X.-Y.; Stern, C. L.; Malliakas, C. D.; Snurr, R. Q.; Stoddart, J. F. *Nat. Chem.* **2024**, *16*, 1982–1988.

10. a) Bezzu, C. G.; Carta, M.; Tonkins, A.; Jansen, J. C.; Bernardo, P.; Bazzarelli, F.; McKeown, N. B. *Adv. Mater.* **2012**, *24*, 5930–5933; b) Zhu, K.; Kamochi, K.; Kodama, T.; Tobisu, M.; Amaya, T. *Chem. Sci.* **2020**, *11*, 9604–9610; c) Park, J.; Kim, J.; Yun, H.-S.; Paik, M. J.; Noh, E.; Mun, H. J.; Kim, M. G.; Shin, T. J.; Seok, S. Il *Nature* **2023**, *616*, 724–730; d) Chen, Y.; Xu, J.; Gao, P. *Org. Chem. Front.* **2024**, *11*, 508–539; e) Okubo, K.; Oka, K.; Tsuchiya, K.; Tomimoto, A.; Tohnai, N. *Angew. Chem. Int. Ed.* **2024**, *63*, e202400475.

11. a) Swager, T. M. *Acc. Chem. Res.* **2008**, *41*, 1181–1189; b) Chong, J. H.; MacLachlan, M. J. *Chem. Soc. Rev.* **2009**, *38*, 3301–3315; c) Zhao, L.; Li, Z.; Wirth, T. *Chem. Lett.* **2010**, *39*, 658–667; d) Chen, C.-F.; Han, Y. *Acc. Chem. Res.* **2018**, *51*, 2093–2106; e) Ueberricke, L.; Mastalerz, M. *Chem. Rec.* **2021**, *21*, 558–573.

12. a) Wittig, G.; Schoch, W. *Liebigs Ann. Chem.* **1971**, *749*, 38–48; b) Dyker, G.; Körning, J.; Jones, P. G.; Bubenitschek, P. *Angew. Chem. Int. Ed. Engl.* **1993**, *32*, 1733–1735; c) Dyker, G.; Körning, J.; Bubenitschek, P.; Jones, P. G. *Liebigs Ann. Recueil* **1997**, 203–209; d) Hackfort, T.; Kuck, D. *Eur. J. Org. Chem.* **1999**, 2867–2878.

13. Debroy, P.; Lindeman, S. V.; Rathore, R. *Org. Lett.* **2007**, *9*, 4091–4094.

14. Kawai, S.; Krejčí, O.; Nishiuchi, T.; Sahara, K.; Kodama, T.; Pawlak, R.; Meyer, E.; Kubo, T.; Foster, A. S. *Sci. Adv.* **2020**, *6*, eaay8913.

15. Kato, K.; Seto, N.; Chida, K.; Yoshii, T.; Mizuno, M.; Nishihara, H.; Ohtani, S.; Ogoshi, T. *Bull. Chem. Soc. Jpn.* **2022**, *95*, 1296–1302.

16. a) Kubo, T.; Miyazaki, S.; Kodama, T.; Aoba, M.; Hirao, Y.; Kurata, H. *Chem. Commun.* **2015**, *51*, 3801–3803; b) Kodama, T.; Hirao, Y.; Nishiuchi, T.; Kubo, T. *ChemPlusChem* **2017**, *82*, 1006–1009; c) Kodama, T.; Miyazaki, S.; Kubo, T. *ChemPlusChem* **2019**, *84*, 599–602; d) Lv, L.; Roberts, J.; Xiao, C.; Jia, Z.; Jiang, W.; Zhang, G.; Risko, C.; Zhang, L. *Chem. Sci.* **2019**, *10*, 4951–4958; e) Lv, L.; Sun, W.; Jia, Z.; Zhang, G.; Wang, F.; Tan, Z.; Zhang, L. *Mater. Chem. Front.* **2020**, *4*, 3539–3545; f) Kato, K.; Uchida, Y.; Kaneda, T.; Tachibana, T.; Ohtani, S.; Ogoshi, T. *Chem. Asian J.* **2024**, *19*, e202400080.

17. a) Kato, K.; Tanaka, S.; Seto, N.; Wada, K.; Gon, M.; Fa, S.; Ohtani, S.; Tanaka, K.; Ogoshi, T. *Chem Commun.* **2023**, *59*, 7080–7083; b) Kato, K.; Tanaka, K.; Kaneda, T.; Ohtani, S.; Ogoshi, T. *Chem. Eur. J.* **2024**, *30*, e202402828.

18. For a hexa-*tert*-butylated [3.3.3]propellane, two- and three-fold formylation has recently been reported: a) Kodama, T.; Aoba, M.; Hirao, Y.; Rivero, S. M.; Casado, J.;

Kubo, T. *Angew. Chem. Int. Ed.* **2022**, *61*, e202200688; b) Kodama, T.; Hirao, Y.; Kubo, T. *Precis. Chem.* **2023**, *1*, 183–191.

19. Organometal reagents of functional π-systems are effective for nucleophilic addition to carbonyl groups: a) Fujimoto, K.; Yorimitsu, H.; Osuka, A. *Eur. J. Org. Chem.* **2014**, 4327–4334; b) Niko, Y.; Sasaki, S.; Narushima, K.; Sharma, D. K.; Vacha, M.; Konishi, G.-i. *J. Org. Chem.* **2015**, *80*, 10794 − 10805; c) Kato, K.; Kim, W.; Kim, D.; Yorimitsu, H.; Osuka, A. *Chem. Eur. J.* **2016**, *22*, 7041–7045; d) Kato, K.; Furukawa, K.; Osuka, A. *Angew. Chem. Int. Ed.* **2018**, *57*, 9491 –9494.

20. Vilsmeier, A.; Haack, A. *Ber.* **1927**, *60*, 119–122.

21. Duff, J. C.; Bills, E. J. *J. Chem. Soc.* **1932**, 1987–1988.

22. a) Rieche, A.; Gross, H.; Höft, E. *Chem. Ber.* **1960**, *93*, 88–94; b) Yamato, T.; Miyazawa, A.; Tashiro, M. *J. Chem. Soc. Perkin Trans. 1* **1993**, 3127–3137; c) Unikela, K. S.; Merner, B. L.; Ghasemabadi, P. G.; Warford, C. C.; Qiu, C. S.; Dawe, L. N.; Zhao, Y.; Bodwell, G. J. *Eur. J. Org. Chem.* **2019**, 4546–4560; d) Kato, K.; Ohtani, S.; Gon, M.; Tanaka, K.; Ogoshi, T. *Chem. Sci.* **2022**, *13*, 13147–13152.

23. a) Zhang, G.-W.; Li, P.-F.; Meng, Z.; Wang, H.-X.; Han, Y.; Chen, C.-F. *Angew. Chem. Int. Ed.* **2016**, *55*, 5304–5308; b) Wang, J.-Q.; Li, J.; Zhang, G.-W.; Chen, C.-F. *J. Org. Chem.* **2018**, *83*, 11532–11540.

24. a) Taylor, R. G. D.; Bezzu, C. G.; Carta, M.; Msayib, K. J.; Walker, J.; Short, R.; Kariuki, B. M.; McKeown, N. B. *Chem. Eur. J.* **2016**, *22*, 2466–2472; b) Kato, K.; Hiroi, T.; Seto, N.; Ohtani, S.; Ogoshi, T. *Chem. Lett.* **2022**, *51*, 975–977; c) Chen, Y.; Zhao, Y.; Zhao, Y.; Chen, X.; Liu, X.; Li, L.; Cao, D.; Wang, S.; Zhang, L. *Angew. Chem. Int. Ed.* **2024**, *63*, e202401706; d) Kato, K.; Okada, S.; Mizuno, M.; Seto, N.; Iwano, R.; Ohtani, S.; Ogoshi, T. *ChemRxiv*, **2025**, DOI: 10.26434/chemrxiv-2025-pkb6x.